Geophysical Research Letters

RESEARCH LETTER
10.1029/2019GL086768

Ongoing Dispersal of the 7 August 2019 Pumice Raft From the Tonga Arc in the Southwestern Pacific Ocean

Martin Jutzeler[1], Robert Marsh[2], Erik van Sebille[3], Tushar Mittal[4], Rebecca J. Carey[1], Kristen E. Fauria[5], Michael Manga[4], and Jocelyn McPhie[1]

[1]Earth Sciences and CODES, University of Tasmania, Hobart, Australia, [2]School of Ocean and Earth Science, University of Southampton, Southampton, UK, [3]Institute for Marine and Atmospheric research, Utrecht University, Utrecht, Netherlands, [4]Department of Earth and Planetary Science, University of California, Berkeley, CA, USA, [5]Department of Earth and Environmental Sciences, Vanderbilt University, Nashville, TN, USA

Abstract On the 7 August 2019, a 195 km^2 raft of andesitic pumice was produced at 200 m below sea level at an unnamed submarine volcano in the Tonga Islands (Southwest Pacific Ocean). Drifting chiefly westward, the raft reached the Fiji Islands on the 19 September. Yachts that crossed the raft as early as 2 days post-eruption provided an outstanding data set of raft characteristics and pristine samples. Further, exceptional tracking of raft dispersal by satellite images allows us to contrast virtual particle tracking methods with ocean model currents to explore the relative influence of surface currents, wind, and wave action on pumice flotsam dispersal over up to 2 years. Attenuation of ocean waves by large and compact pumice rafts appears to reduce the effect of Stokes drift. The coupling of real-time satellite observations with oceanographic Lagrangian simulations allows near-real time forecasting for global maritime hazard mitigation.

Plain Language Summary Although 70% of volcanism occurs underwater, submarine eruptions are seldom witnessed owing to their remoteness and absence of technologies enabling their detection. On the 7 August 2019, a submarine volcanic eruption 200 m below sea level in the Tonga Islands formed a 195 km^2 pumice raft. The raft was first encountered and sampled by yacht crews, and is visible on satellite images. Pumice rafts are dispersed by ocean currents, wind, and waves, and can cross entire oceans or get stranded on coasts. After 7 weeks of dispersal, the pumice raft reached the Fiji Islands, and a fraction continued its westward route toward Vanuatu and eastern Australia. Excellent imaging of the raft by satellites permitted reconstruction of daily raft dispersal for the first 8 weeks. Here we show that drift calculations, including components of ocean current, wind, and wave action, can usefully forecast raft dispersal. We tested and tuned these drift calculations by comparing the simulated drift with daily satellite images of the raft. Further, a combination of satellite images and drift calculations based on oceanographic models were used for maritime hazard mitigation in near-real time.

Key Points:
- A >30 million m^3 pumice raft formed at an unnamed volcano in Tonga midday on the 7 August 2019 and was dispersed by ocean currents and wind
- Forecasts of pumice raft dispersal, based on particle drift with model currents, winds, and waves, are evaluated with daily satellite images
- Stokes drift does not improve short-term predictions on large and compact pumice rafts because these rafts attenuate ocean waves

Supporting Information:
- Supporting Information S1

Correspondence to:
M. Jutzeler,
jutzeler@gmail.com

Citation:
Jutzeler, M., Marsh, R., van Sebille, E., Mittal, T., Carey, R. J., Fauria, K. E., et al. (2020). Ongoing dispersal of the 7 August 2019 pumice raft from the Tonga arc in the southwestern Pacific Ocean. *Geophysical Research Letters*, *47*, e1701121. https://doi.org/10.1029/2019GL086768

Received 27 SEP 2019
Accepted 13 FEB 2020
Accepted article online 18 FEB 2020

Introduction

On the 9 August 2019, two yacht crews had the serendipity of being the first to encounter and report on a newly formed pumice raft between Tonga and Fiji in the Southwest Pacific. This 195 km^2 raft extended to the horizon and consisted of a 15–30 cm thick layer of freshly erupted pumice clasts, implying a minimum estimated volume of 30 million m^3 (Figure 1). The pumice raft was 2 days old, and erupted from a submarine caldera volcano at ca. 200 m below sea level (mbsl), 50 km northwest of Vava'u in the Kingdom of Tonga (Global Volcanism Program, 2019), part of the Tonga-Kermadec arc.

The initial raft progressively dispersed into multiple smaller rafts, some of which were stranded on Lakeba Island (Lau group) on the 2 September, 460 km west from their source. Hundreds of small (<0.1 km × <2 km) rafts reached the main Fiji Islands on the 19 September, and most of them got stranded on the eastern shores of the Yasawa Islands for >2 months until being released back in the open ocean to continue their northwestward route.

Here we show that the remaining rafts will continue their westward route through the South Equatorial Current, and a fraction of them is likely to reach the eastern shores of mainland Australia in about middle to late 2020. To date, the transit of this pumice raft has provided an exceptional opportunity to study controls

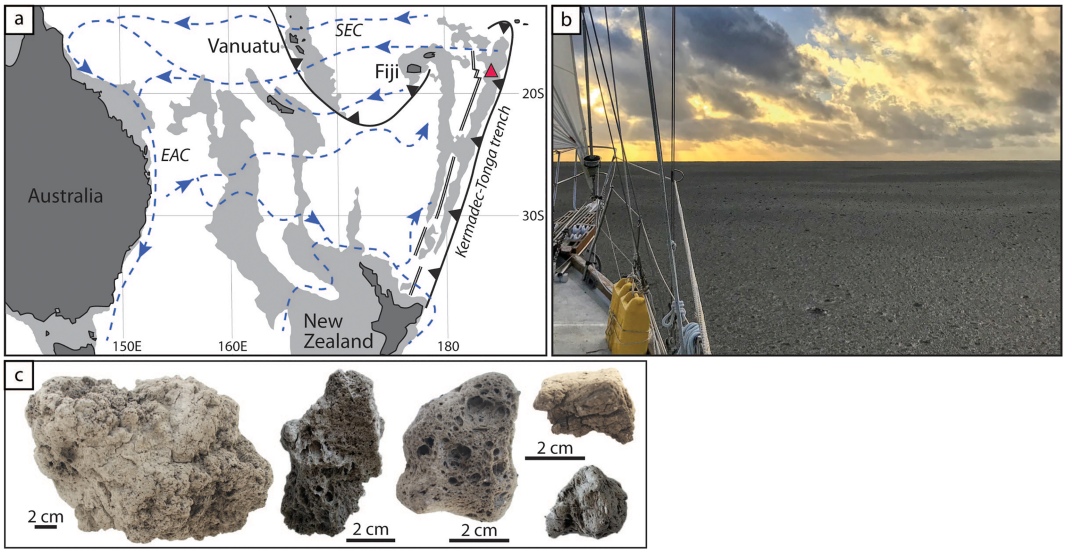

Figure 1. (a) Tectonic, oceanographic, and bathymetric map simplified after Collins (2002) and Wijeratne et al. (2018); gray areas for 2,000 mbsl contour; dashed blue line for ocean currents, black lines for subduction zones; double black lines for mid-ocean ridges; volcano as red triangle; SEC for South Equatorial Current; EAC for East Australian Current, (b) SV *Finely Finished* sailing across the 2-day old pumice raft at sunset. The waves are strongly attenuated (at least half their height) by the raft. (c) Pumice samples collected by various yacht crews, including (from left to right) coarse clast with polyhedral joints; clast with quenched rim enhanced by grading in vesicularity from rim (top) to core (base); subrounded clast; subangular clasts with polyhedral joints. Photo courtesy Shannon Lenz.

on dispersal, because low cloud cover permitted almost daily observation of the raft through satellite imagery, augmented by observations and sampling by yacht crews.

After formation, pumice rafts thin by areal dispersion, pumice abrasion, and loss of pumice clasts through progressive waterlogging and overloading by biota, and/or get stranded on coasts and islands (Bryan et al., 2012; Jutzeler et al., 2014). Pumice can float for months to many years (Fauria et al., 2017; Fauria & Manga, 2018; Whitham & Sparks, 1986), and forms an unusual flotsam that has been recognized since the Antiquity (Fouqué, 1879; Hurlbut & Verbeek, 1887; Oppenheimer, 2003; Sutherland, 1965).

Like other flotsam, pumice clasts move by combination of draft (ocean currents), windage (wind), and Stokes drift (waves), by which oscillatory motion induces a net drift in the direction of wave propagation (Bryan et al., 2004; Jutzeler et al., 2014). However, the effects of these three dispersal factors are poorly constrained for pumice rafts, and likely vary throughout the life of a raft, depending on its size and thickness, as well as size and buoyancy of its pumice clasts, and prevailing weather conditions.

Largely unrecognized, hazards from pumice rafts range from local nuisance to serious effects on local and regional economies. Large pumice rafts can block harbors for months and divert maritime traffic (Hurlbut & Verbeek, 1887; Jutzeler et al., 2014; Oppenheimer, 2003; Sigurdsson et al., 1982). Pumice clasts can obstruct water intakes. Moreover, pumice clasts are abrasive and known to scrape hulls and damage propellers. Rafts block sunlight which impact sea life, air-sea heat and gas exchange in the upper ocean; rafts that get stuck in shallow water for extended times likely kill most organisms underneath the raft, as witnessed by many in Fiji. Further, the tourism industry may suffer from beaches being inaccessible or degraded by abundant flotsam.

First alerted by the Rescue and Co-Operation Centre New Zealand (RCCNZ) on the 14 August, we immediately assessed raft dispersal and its source vent using satellite images and oceanographic particle tracking models. Biweekly hazard maps were communicated to RCCNZ, the Maritime Safety Authority of Fiji, and key local individuals for dissemination to the yachting, shipping, and fishing communities via social media and word of mouth. This strategy successfully prevented further vessels from encountering the pumice raft, and facilitated contact with sailing crews for information on the raft and samples.

Modeling pumice raft dispersal was previously performed using surface velocity fields for the 2001 raft from the same unnamed volcano (Bryan et al., 2004) and ocean model hindcast currents for the 2012 Havre raft (Jutzeler et al., 2014). The present study is the first to statistically predict the dispersal of an active pumice raft by computing particle trajectories using Parcels particle tracking software (Delandmeter & van Sebille, 2019) in combination with openly available ocean current data from the Copernicus Marine Environmental Monitoring Service (CMEMS) for short-term (1 month) and long-term (2 years) simulations.

Methods

Satellite Surveillance

Freely available moderate resolution natural reflectance images captured by sun-synchronous satellites such as MODIS Terra and Aqua (250-m pixel), Sentinel-3 (300-m pixel), and Suomi-VIIRS (375-m pixel) are very efficient for tracking large pumice rafts in real time. Their sequential passing over of the same area within a few hours daily increases the chances of identifying rafts in clear to partly cloudy weather. High-resolution satellite images from Sentinel-2 (10-m pixel) and LANDSAT-8 (30-m pixel) are excellent for raft tracking and identification of small features, although imaging frequency is ca. 3 days. The radar-equipped Sentinel-1 satellite (10-m pixel) in *Interferometric Wide Swath* mode (single VV polarization) is excellent at identifying nondilute rafts in any weather, although imaging frequency is low. Coastal ocean images obtained from the commercial fleet of *Planet* satellites are down to 0.8-m pixel. Our satellite image analysis and dispersal maps use combined data from all these satellites.

Oceanographic Simulations

We conducted short-term (1 month) forecast and long-term (2 year) hindcast simulations based on data from CMEMS (see acknowledgments and supporting information Text S1). These data include ocean currents and Stokes drift on 1/12° horizontal grid, as well as wind data on 1/4° horizontal grid, which each provide different dispersal patterns (Onink et al., 2019). Particles were released at (18.307°S 174.395°W) on the 7 August. Particle trajectories were calculated using Parcels (Delandmeter & van Sebille, 2019) (OceanParcels.org), a rapid, customizable framework for Lagrangian particle tracking simulations using output from Ocean Circulation models. The full code of these simulations is available at https://github.com/OceanParcels/PumiceEvent.

A key factor in pumice dispersal is windage, included as a fraction of the wind vector from the ocean model simulation. If a typical value of 1% windage is added to the surface current vector (e.g., Putman et al., 2018), then for usual wind speeds 5–10 m/s (trade winds) and current speeds 0.1–0.2 m/s (surface flow in the tropics), windage is about half the current speed. While previous estimates of pumice drift incorporated this wind percentage (around 50%) of current speed (Bryan et al., 2004), we more accurately include a windage effect that is independent of the current.

Data and Results

Close Encounter With the New Pumice Raft

On the afternoon and evening of the 9 August (all times are local, UTC + 13), SV *Finely Finished* and MY *Olive* crossed and sampled the main raft only 2 days after the eruption, providing invaluable information on the products of this submarine eruption (Figures 1, S1–S6; Movies S1 and S2). The crews' logbooks, photos, and videos described the main raft to be a compact, 15–30 cm thick layer of pumice clasts. The diameters of most clasts are a few centimeters, but range 0.3–80 cm. Patchy raft ribbons (elongated rafts) alongside or behind the main raft were composed of small (<1 km), one-clast thick rafts (Figure 2). These measurements combined with the raft area imply a volume of at least 30 million m^3 2 days after the eruption. On the 11 August, SV *Barbarossa* crossed the 2-km-wide main raft (Figure 3a). The reported raft was one-clast thick and predominantly comprised subrounded pumice clasts ca. 6 cm in size, with outliers at 0.2 and 40 cm, matching reports from all vessels that encountered the raft, including SY *Arka* and SY *Roam* on the 14 and 15 August, respectively (Figure 3a). All sampled pumice clasts are pale grey to pale brown, include coarse phenocrysts, and are highly vesicular (Figure 1). Chemically, the pumice is andesitic (Table S1), less evolved than the 2001 dacite (Bryan et al., 2004). The pumice clasts collected over the first week are well rounded to subangular, and display polyhedral joints, weak cauliflower texture, and a gradational rim-to-core increase in

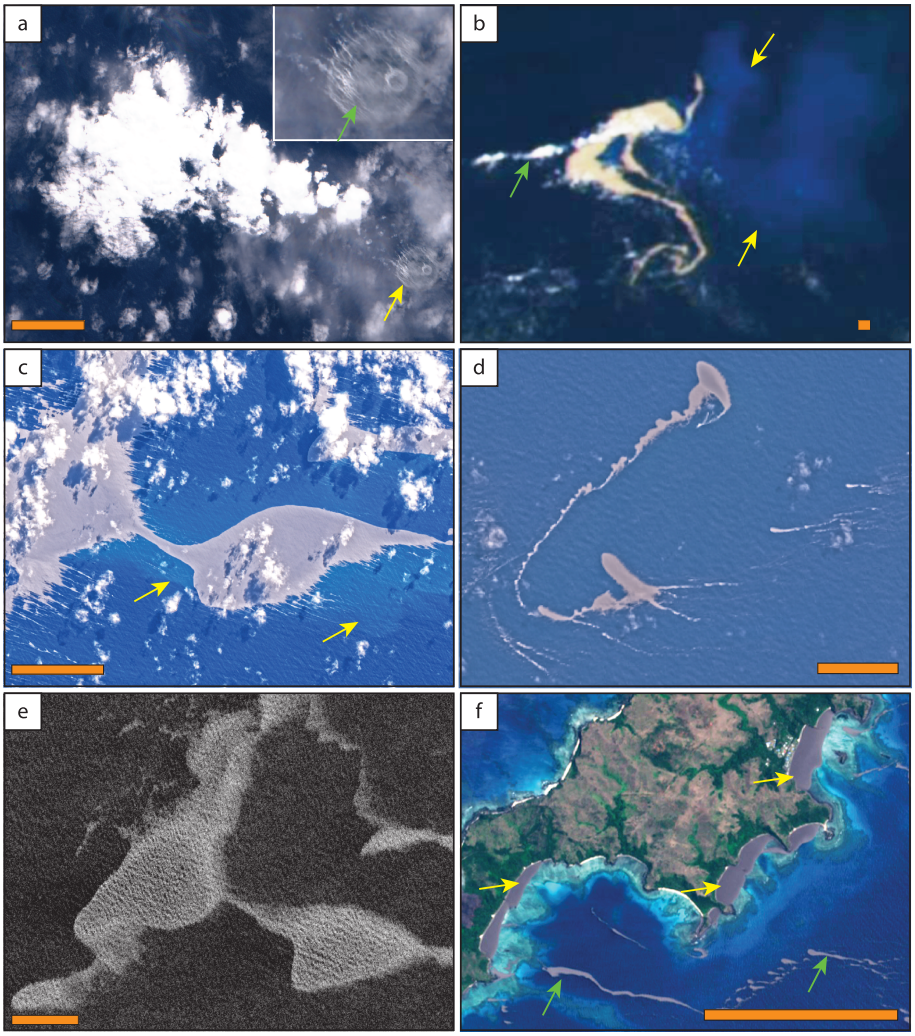

Figure 2. Satellite images of the pumice raft; orange scale bars are 2 km. (a) Sentinel-2 (10-m pixel) on the 7 August 2019 with two billowing rings (yellow arrow) and water vapor plume. Inset: close-up of the billowing rings with linear trails of water vapor (green arrow). (b) VIIRS-Suomi (375-m pixel) on the 10 August showing the crescent-shape pumice raft drifting westward. Pale-blue discolored water contains a suspension of glass shards produced by abrasion (yellow arrows). Westward drifting clouds are formed by island effect of the raft (green arrow). (c) Sentinel-2 (10-m pixel) on the 12 August with large raft drifting westward. Frontal edges (left) are sharp, whereas posterior edges are jagged and scale with the swell. Pale-blue discolored water contains suspended glass shards produced by pumice raft abrasion (yellow arrows). (d) Landsat-8 (30-m pixel) on the 21 August. Small rafts have been sheared during eddying, forming ribbons. (e) Sentinel-1 radar (AWS-VV; 10-m pixel) image on the 12 August showing the thick parts of the raft (pale gray-white). This image is taken 5 hr before (c). (f) Sentinel-2 (10-m pixel) on the 29 September showing arrival (green arrows) and stranding (yellow arrows) of rafts nearby Teci village, Yasawa Island, eastern Fiji.

vesicle size typical of water quenching (McPhie et al., 1993) (Figure 1). The average pumice size (2–6 cm) matches the size of clasts that are able to reach the ocean surface from a submarine vent at ~200 mbsl prior to ingesting enough water to sink (Fauria & Manga, 2018) (Text S2; Figure S7).

A Submarine Eruption

This eruption is the first reported activity of this volcano since its pumice-raft forming eruption from a nearby vent in 2001 (Brandl et al., 2019; Bryan et al., 2004; Global Volcanism Program, 2019). Precursory activity included a 5.7 Mw earthquake at 10:01 pm on the 5 August, at 15 km south-southwest of the volcano and 10 km depth, followed by six events of around magnitude 4 over the next 2 days (Brandl et al., 2019; International Seismological Centre, 2019) (Figure S8). A Sentinel-1 satellite image on the 6 August,

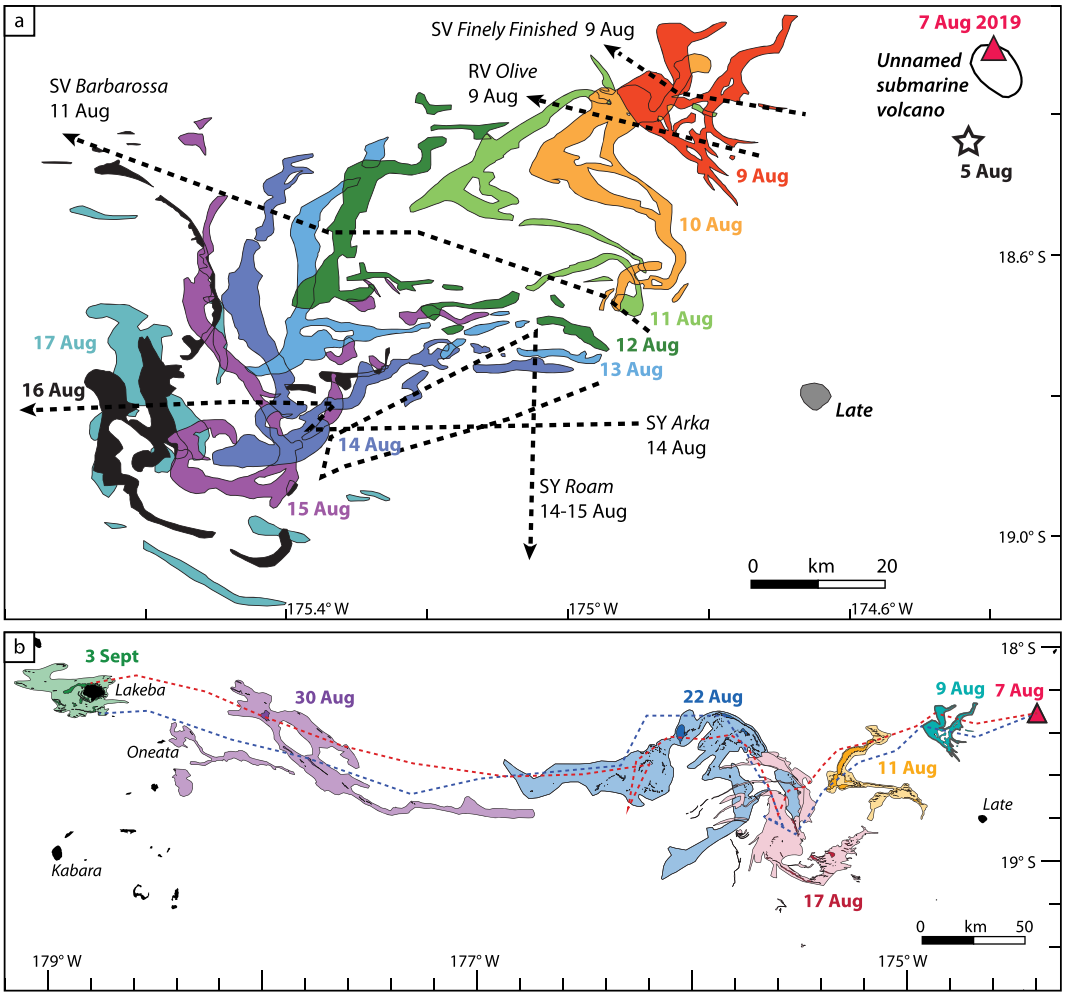

Figure 3. Time-series of raft dispersal selected from 118 satellite images. (a) First days of raft dispersal. The raft dispersed southwestward from the vent (red triangle) and got entrained into an ocean loop or eddy on the 15–17 August. Five yachts crossed the early raft (dashed lines). Caldera margin, solid black line; precursory earthquake, white star. (b) Raft dispersal with high-resolution Sentinel-2 and -3. Large rafts are bright, dilute and spread rafts are pale. Two dispersal trails (blue and red dashed lines) show daily dispersal of two parts of the raft that became separated on the 17 August.

7:07 pm showed no surficial evidence of eruptive activity, and no activity has been imaged since at least 2013 (Movies S3 and S4). High-resolution Sentinel-2 satellite imagery at 11:01 am on the 7 August shows two concentric rings of 225 and 1,150 m diameter emerging from a point source centered at (18.307°S 174.395°W) (Figure 2). This point source corresponds to a 200 mbsl bathymetric high on the northernmost rim of the 8 × 5 km, 700 mbsl unnamed submarine caldera volcano (Brandl et al., 2019; Global Volcanism Program, 2019; Taylor, 2012). This vent location is 1.5 km northwest from the supposed 2001 eruption site and situated on the same broad bathymetric high and on the caldera rim (Figure S9). The two rings strongly resemble breaching of billowing underwater eruption columns or steam cupolas generated during shallow submarine eruptions (Kokelaar & Durant, 1983; Somoza et al., 2017). No pumice raft is visible in the satellite image of the rings (pixel size 10 m), therefore pumice raft formation occurred subsequently. Raft velocity on the 9 August suggests pumice raft formation at midday on the 7 August 2019 (Text S3).

We observed ca. 10 m wide, white linear trails scattered above the concentric rings that we interpret to be condensed water vapor blown northwestward by surface wind (Figure 2a). This water vapor was likely derived from very coarse, warm pumice clasts and/or fluid that breached the water surface (Reynolds et al., 1980). A low-altitude, white atmospheric plume fanned out at 2–11 km northwest (downwind) from

the inferred vent. This plume, presumably made of condensed water vapor, is attributed to the eruptive pulse that produced the largest billowing ring (Figure 2). No ash-rich or SO_2-rich (Sentinel-5 satellite) eruption plume is observed in any of the satellite images. The atmospheric wind profile (Figure S10) and plume direction constrain a plume height <1,000 m.

Available satellite images show minor activity at the vent at least on the 9 and 11 August, with emission of a trail of pale blue-green discolored water and a delayed, small (<1 km^2) and dilute raft at 2–5 km from the vent (11 August). The eruption style cannot be ascertained without further textural and chemical analyses of the pumice clasts, a post-eruption bathymetry survey, and seafloor sampling of proximal volcanic products. The first satellite image shows a strongly irregular-shaped raft, suggesting successive raft-forming eruption pulses. The low viscosity of the erupted andesite hinders fragmentation in the conduit (Text S4) so that clasts may be generated by quenching in the ocean, consistent with some of the observed textures.

Pumice Raft Formation and Dispersal

The edges of the raft were digitized from georeferenced satellite images imported into QGIS software. Our time-series from the 9 August to the 3 September includes 61 satellite passes over the raft, allowing precise reporting of its geometry and areal distribution (Figure 3). The raft drifted 5–54.5 km/day (22.8 km/day average, matching global dispersal speeds; Jutzeler et al., 2014) westward overall but was entrained into ocean loops or eddies and changed direction (Figure 3; Text S5). The early raft was 195 km^2 (9 August) and sailing crew observations of raft thinning from 30–50 cm to one-clast thick (5 cm) from the 9 to the 11 August imply areal dispersal and pumice abrasion (Jutzeler et al., 2014). Over the next weeks of dispersal, the raft broke up into hundreds of small (<1 km^2) rafts, which covered an area of <1,600 km^2 on the 30 August, not including rafts <10 m. Ribbons tend to get segmented into lenses of same wavelength and orientation as the swell (Figure 2c) suggesting that Stokes drift actively contributes to breaking up rafts. The raft passed over Oneata's lagoon and then stranded on Lakeba Island for several days until continuing its westward route toward Fiji. On the 22–26 September, the raft passed through the two main Fiji Islands and most of the raft got stranded 60 km to the west, on the Yasawa Islands (Figure 2f). A few episodes of wind changes allowed fractions of the raft to be released back into the ocean; the shores were eventually cleared on the 29 December (Text S4; Figures S11–S13).

Over the first two weeks of drifting, low-level cloud trails formed above the large (>6 km) raft and often extended downstream (Figure 2b). We infer that these clouds formed by retention of solar radiation on the rafted pumice, favoring evaporation of sea water, similar to an island effect (Yang et al., 2008). This implies that pumice rafts, if big enough, can create their own microclimate.

Degradation of the Raft Through Mechanical Abrasion

Rafted pumice clasts undergo continuous mechanical abrasion by the constant movement of waves and swell causing clasts to move past each other. All sailing crews reported intense clinking noises emitted from the raft. Many of the pumice clasts were subrounded on day 2 of dispersal, and rounded on day 4, attesting to their rapid abrasion (Jutzeler et al., 2017) and thus decrease in raft volume (Figure 1). Satellite images show further evidence of significant clast abrasion as seen in the immense pale-blue discolored water patches that envelope and follow the largest rafts for several weeks post eruption (Figure 2). This pale-blue discolored water is not connected to the submarine eruption plume (Mantas et al., 2011), and likely consists of a fine suspension of glass shards generated by abrasion in the raft, in addition to isolated sinking pumice clasts that will eventually settle to the seafloor (Jutzeler et al., 2014; Jutzeler et al., 2017). Further, blockage of the raft on the eastern shores of the Yasawa Islands for >2 months reveal areal shrinking of the rafts by stranding and/or abrasion by surf. The volume loss of pumice by waterlogging is difficult to calculate without seafloor samples. Sampled pumices from week 1 of dispersal show subangular to rounded pumice clasts, for a minimum volume loss of 10 vol.% (Jutzeler et al., 2014), equivalent to 3 million m^3. Two yacht crews mentioned a pronounced smell of sulfur crossing the rafts on days 2 and 6 of raft dispersal. Sulfur dioxide and hydrogen sulfide are volcanic gases that are trapped within isolated pore space of pumice. Its detection by the crews far from the vent and several days after the eruption attests of its release by fragmentation of the delicate pumice vesicle walls by rafting-induced abrasion, rather than originating directly from an eruption plume that would have been rapidly dispersed by surface wind.

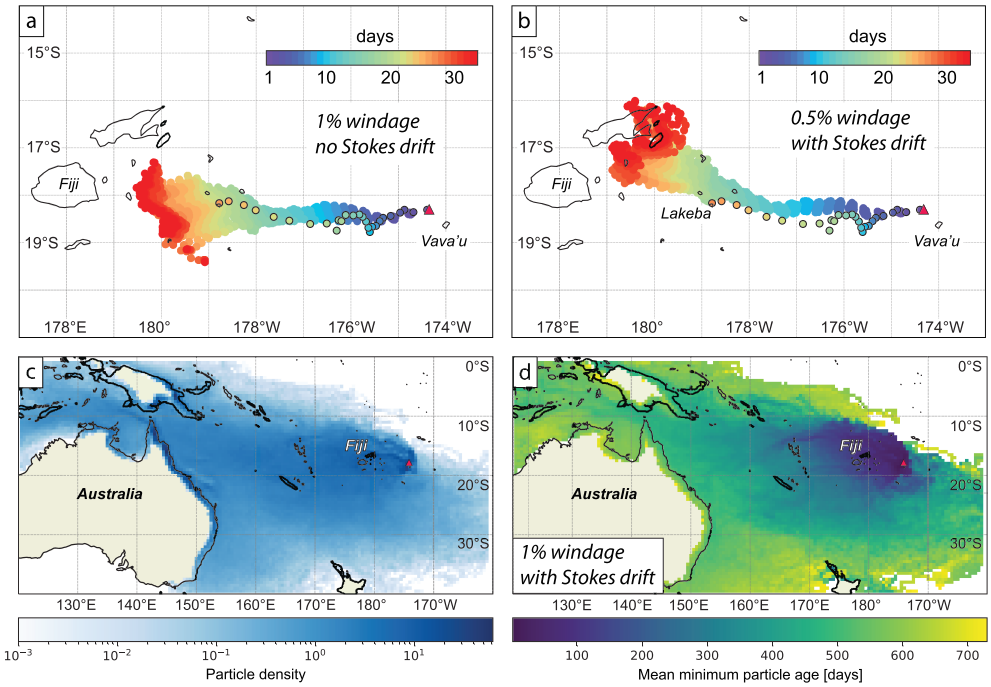

Figure 4. Oceanographic simulations of raft dispersal. (a and b) One-month simulation with Parcels (unrimmed circles) compared with satellite imagery (black-rimmed circles). (c and d) Two-year simulation with Parcels for releases on each 7 August of the years 2000–2013, with 1% windage and including Stokes drift. (c) Cumulative distributions of particle concentration as grid-cell fraction. (d) Cumulative distributions of minimum days adrift. Red triangle for source volcano.

Forecasting Raft Dispersal by Ocean Currents, Waves, and Winds

We initially simulated dispersal of the raft for 1 month, under a range of windage values and Stokes drift (Figures 4a, 4b, and S14). The dispersal simulation reproduces actual raft drift relatively well. The simulation shows a very good match in westward dispersal direction, and includes sinuosities that broadly but not completely match those observed in satellite images. Simulated dispersion matches satellite data for the first week, but then becomes 20–30% faster over the following weeks. Among the four simulations presented (Figure S14), the best match is with a 1% windage and no Stokes drift (Figure 4a).

The long-term simulations show predominant westward dispersal by the South Equatorial Current, assisted by south-easterly trade winds (Figures 4, S15–S17). Earliest arrival times on the eastern Australian coast fall in the range 300–540 days (Figure 4a), or March 2020 to January 2021, matching raft dispersal rates in this region (Bryan et al., 2004; Jutzeler et al., 2014). There is a trend for generally later arrival times as we move southward along the eastern seaboard of Australia. These averages "hide" considerable interannual variability in the hindcast (Figure S17), most evident in the wide meridional spread and the common occurrence of an additional eastward dispersal. Approaching the eastern coast of Australia, particles move either northward and further westward through the Indonesian Archipelago, or southward with the East Australian Current. These results are sensitive to the choice of windage parameter, with higher windages leading to a generally more westward drift. Adding of Stokes drift led to a slightly more northward pathway. In all cases, however, the modeled plume was transported faster than in the satellite observations (Figures 4a, 4b, and S14). Of consequence here, we note looping of the observed trajectory in the longitude range 175–177°W during days 5–15, broadly consistent with inertial motion at this latitude under a sudden change in winds. The discrepancy between simulated and observed drift may thus be a consequence of inertial currents that are unresolved in the CMEMS data, although additional unresolved motion may be attributed to small-scale eddies. The El Niño–Southern Oscillation was relatively neutral at time of raft dispersal (see https://www.esrl.noaa.gov/psd/enso/mei/). We therefore expect the dispersal pathways to be similar to e.g., 2003–2006. For the model hindcast, we consider the cumulative coverage over 14 years (2000–2013) to be representative of much of the variability in ocean currents.

Discussion and Conclusion

The application of the Parcels short-term simulation to the well-constrained trajectories of the pumice raft is a rare opportunity to explore windage and Stokes drift parametrizations. The windage for pumice is likely typical for semisubmerged objects, such as pelagic *Sargassum* in the equatorial and tropical Atlantic, for which 1% windage has also been estimated (Putman et al., 2018). A refined understanding of windage would thus be of broad utility in tracking buoyant material throughout the global ocean (Durgadoo et al., 2019). Overall, the simulated short-term trajectories accurately match the pathway of raft dispersal, although dispersal speed is overestimated by 20–30% after week 1. This discrepancy in dispersal speed is consistent with unresolved inertial motion at this latitude, or entrainment of rafts into a small unforecasted eddy, either of which might explain the looping trajectory and delayed westward dispersal over the 15–17 August (Figures 3 and 4). Stranding on Lakeba (days) and Yasawa Islands (months) strongly delayed dispersal of large parts of the raft; the stranding time and ability for a pumice raft to reenter the open ocean is difficult to forecast.

The addition of Stokes drift does not improve the short-term simulations. Stokes drift is computed from wave characteristics for the open ocean, and these data may not be appropriate for large and compact pumice rafts, because the local wave height is strongly attenuated by the raft, which reduces wind drag on the ocean surface, similar to an oil slick (Shen et al., 2019; Zhang et al., 2015). SV *Finely Finished* crew reported within-raft waves being at least half-sized and much smoother compared to waves in the adjacent free ocean (Figure 1a; Movies S1 and S2). However, we expect the Stokes drift to be substantially attenuated only for large (>1 km^2) and compact rafts. Therefore, short-term simulations should not include Stokes drift as a dispersal component for large rafts over the first weeks of drifting, but ought to be included in longer-term simulations and/or when simulating small and dilute rafts.

The tuning of windage is more difficult to assess. The wind velocity in the studied area was relatively high (7 m/s average), and variations in wind speed and direction occurred often (Figure S18). Windage is an important component of raft dispersal (Bryan et al., 2004), and depends on raft area and thickness, and pumice buoyancy. Variations in windage from 0.5% to 1% have strong effects on the short-term simulation by affecting the overall dispersal of the raft after week 3 (Figures 4 and S14), highlighting the necessity of periodic satellite imagery to ascertain the raft heading and to tune its relative windage component.

Current satellite technology allowed tracking of large pumice rafts daily (weather permitting), enabling (1) tuning of oceanographic simulations for windage and Stokes drift and (2) fast production of hazard maps for New Zealand and Fiji authorities for dissemination to the yachting, shipping, and fishing communities.

Acknowledgments
We thank the *Rescue and Co-Operation Centre New Zealand*, the *Maritime Safety Authority of Fiji*, and Greg Just (Vava'u) for dissemination of our hazard maps and enabling communication with yacht crews. We are grateful to yacht crews for samples and information; we are quite envious of their extraordinary experience: Rachel (MY *Olive*), Patricia and Silvio (SV *Barbarossa*), Michael and Larissa (SY *Roam*), Shannon and Tom (SV *Finely Finished*), Jim (SV *Bright Moments*), Diego and crew (SY *Arka*), and Kostya (SV *Ponyo*). We thank N. Kumar for sampling on Viti Levu and organizing sample postage and F. Ikegami for support with QGIS. We acknowledge funding for M.M. and T.M. from NSF grant EAR#1615203. We thank two anonymous reviewers and E. Klemetti for their comments. The Parcels/CMEMS simulations were performed on the Dutch national e-infrastructure with support of SURF Cooperative (project-16371). The code for the Parcels simulations is available online (https://github.com/OceanParcels/PumiceEvent). This paper uses data from: http://marine.copernicus.eu/services-portfolio/access-to-products/?option=com_csw&view=details&product_id=GLOBAL_ANALYSIS_FORECAST_PHY_001_024; http://marine.copernicus.eu/services-portfolio/access-to-products/?option=com_csw&view=details&product_id=GLOBAL_ANALYSIS_FORECAST_WAV_001_027; http://marine.copernicus.eu/services-portfolio/access-to-products/?option=com_csw&view=details&product_id=WIND_GLO_WIND_L4_NRT_OBSERVATIONS_012_004. Interested users can access our data through contacting MJ.

References

Brandl, P. A., Schmid, F., Augustin, N., Grevemeyer, I., Arculus, R. J., Devey, C. W., et al. (2019). The 6–8 Aug 2019 eruption of 'Volcano F' in the Tofua Arc, Tonga. *Journal of Volcanology and Geothermal Research*, *390*, 106695. https://doi.org/10.1016/j.jvolgeores.2019.106695

Bryan, S. E., Cook, A. G., Evans, J. P., Colls, P. W., Wells, M. G., Lawrence, M. G., et al. (2004). Pumice rafting and faunal dispersion during 2001-2002 in the Southwest Pacific: Record of a dacitic submarine explosive eruption from Tonga. *Earth and Planetary Science Letters*, *227*, 135–154.

Bryan, S. E., Cook, A. G., Evans, J. P., Hebden, K., Hurrey, L., Colls, P., et al. (2012). Rapid, long-distance dispersal by pumice rafting. *Plos One*, *7*, e40583. https://doi.org/10.1371/journal.pone.0040583

Collins, W. J. (2002). Nature of extensional accretionary orogens. *Tectonics*, *21*(4), 1024. https://doi.org/10.1029/2000TC001272

Delandmeter, P., & van Sebille, E. (2019). The Parcels v2. 0 Lagrangian framework: New field interpolation schemes. *Geoscientific Model Development*, *12*(8), 3571–3584.

Durgadoo, J. V., Biastoch, A., New, A. L., Rühs, S., Nurser, A. J. G., Drillet, Y., & Bidlot, J.-R. (2019). Strategies for simulating the drift of marine debris. *Journal of Operational Oceanography*, *10*, 1–12.

Fauria, K. E., & Manga, M. (2018). Pyroclast cooling and saturation in water. *Journal of Volcanology and Geothermal Research*, *362*, 17–31.

Fauria, K. E., Manga, M., & Wei, Z. (2017). Trapped bubbles keep pumice afloat and gas diffusion makes pumice sink. *Earth and Planetary Science Letters*, *460*, 50–59.

Fouqué, F. A. (1879). *Santorini and its eruptions (translated and annotated by A.R. McBirney, 1998)* (p. 495). Baltimore, MD: John Hopkins University Press.

Global Volcanism Program (2019). Report on unnamed (Tonga). In S. K. Sennert (Ed.), *Weekly Volcanic Activity Report, 14 August-20 August 2019*. Washington, DC: Smithsonian Institution and US Geological Survey.

Hurlbut, G. C., & Verbeek, R. D. M. (1887). Krakatau. *Journal of the American Geographical Society of New York*, *19*, 233–253. https://doi.org/10.2307/196734

International Seismological Centre. (2019). On-line Bulletin. https://doi.org/10.31905/D808B830

Jutzeler, M., Marsh, R., Carey, R. J., White, J. D. L., Talling, P. J., & Karlstrom, L. (2014). On the fate of pumice rafts formed during the 2012 Havre submarine eruption. *Nature Communications*, *5*(1), 3660. https://doi.org/10.1038/ncomms4660

Jutzeler, M., van Sebille, E., & Marsh, R. (2017). Abrasion experiments and hindcast modelling to study tephra dispersal by pumice rafts: Preliminary results., paper presented at AGU Chapman Conference on submarine volcanism, Hobart, Australia.

Kokelaar, B. P., & Durant, G. P. (1983). The submarine eruption and erosion of Surtla (Surtsey), Iceland. *Journal of Volcanology and Geothermal Research*, *19*(3-4), 239–246.

Mantas, V. M., Pereira, A., & Morais, P. V. (2011). Plumes of discolored water of volcanic origin and possible implications for algal communities. The case of the Home Reef eruption of 2006 (Tonga, Southwest Pacific Ocean). *Remote Sensing of Environment*, *115*(6), 1341–1352.

McPhie, J., Doyle, M., & Allen, R. (1993). *Volcanic textures* (p. 198). Hobart, Australia: ARC- Centre of Excellence in Ore Deposits University of Tasmania.

Onink, V., Wichmann, D., Delandmeter, P., & van Sebille, E. (2019). The role of Ekman currents, geostrophy, and stokes drift in the accumulation of floating microplastic. *Journal of Geophysical Research: Oceans*, *124*, 1474–1490. https://doi.org/10.1029/2018JC014547

Oppenheimer, C. (2003). Climatic, environmental and human consequences of the largest known historic eruption; Tambora Volcano (Indonesia) 1815. *Progress in Physical Geography*, *27*(2), 230–259.

Putman, N. F., Goni, G. J., Gramer, L. J., Hu, C., Johns, E. M., Trinanes, J., & Wang, M. (2018). Simulating transport pathways of pelagic Sargassum from the Equatorial Atlantic into the Caribbean Sea. *Progress in oceanography*, *165*, 205–214. https://doi.org/10.1016/j.pocean.2018.06.009

Reynolds, M. A., Best, J. G., & Johnson, R. W. (1980). *1953-57 eruption of Tuluman Volcano; rhyolitic volcanic activity in the northern Bismarck Sea* (p. 44). Port Moresby: Geological Survey of Papua New Guinea.

Shen, H., Perrie, W., & Wu, Y. (2019). Wind drag in oil spilled ocean surface and its impact on wind-driven circulation. *Anthropocene Coasts*, *2*, 244–260.

Sigurdsson, H., Cashdollar, S., & Sparks, S. R. J. (1982). The eruption of Vesuvius in AD 79: Reconstruction from historical and volcanological evidence. *American Journal of Archaeology*, *86*(1), 39–51.

Somoza, L., González, F. J., Barker, S., Madureira, P., Medialdea, T., De Ignacio, C., et al. (2017). Evolution of submarine eruptive activity during the 2011–2012 E l H ierro event as documented by hydroacoustic images and remotely operated vehicle observations. *Geochemistry, Geophysics, Geosystems*, *18*, 3109–3137.

Sutherland, F. L. (1965). Dispersal of pumice, supposedly from the 1962 South Sandwich Islands eruption, on southern Australian shores. *Nature*, *207*(5004), 1332–1335. https://doi.org/10.1038/2071332a0

Taylor, B. (2012) Multibeam bathymetry compilation of the Lau Back-Arc Basin, *Interdisciplinary Earth Data Alliance (IEDA), doi*:https://doi.org/10.1594/IEDA/100063.

Whitham, A. G., & Sparks, R. S. J. (1986). Pumice. *Bulletin of Volcanology*, *48*(4), 209–223. https://doi.org/10.1007/BF01087675

Wijeratne, S., Pattiaratchi, C., & Proctor, R. (2018). Estimates of surface and subsurface boundary current transport around Australia. *Journal of Geophysical Research: Oceans*, *123*, 3444–3466. https://doi.org/10.1029/2017JC013221

Yang, Y., Xie, S.-P., & Hafner, J. (2008). The thermal wake of Kauai Island: Satellite observations and numerical simulations. *Journal of Climate*, *21*(18). https://doi.org/10.1175/2008JCLI1895.1

Zhang, Y., Zhang, J., Wang, Y., Meng, J., & Zhang, X. (2015). The damping model for sea waves covered by oil films of a finite thickness. *Acta Oceanologica Sinica*, *34*, 71–77. https://doi.org/10.1007/s13131-015-0729-1

References From the Supporting Information

Aravena, Á., Cioni, R., Vitturi, M. D. M., & Neri, A. (2018). Conduit stability effects on intensity and steadiness of explosive eruptions. *Scientific reports*, *8*, 4125. https://doi.org/10.1038/s41598-018-22539-8

Batchelor, C. K., & Batchelor, G. (2000). *An introduction to fluid dynamics*. Cambridge, UK: Cambridge University Press.

Giordano, D., Russell, J. K., & Dingwell, D. B. (2008). Viscosity of magmatic liquids: a model. *Earth and Planetary Science Letters*, *271*(1-4), 123–134.

Haxby, W., Melkonian, A., Coplan, J., Chan, S., & Ryan, W. (2010). GeoMapApp freeware software, v. 2.3, *Lamont–Doherty Earth Observatory, Palisades, NY*.

Papale, P., Neri, A., & Macedonio, G. (1998). The role of magma composition and water content in explosive eruptions: 1 Conduit ascent dynamics. *Journal of Volcanology and Geothermal Research*, *87*(1-4), 75–93. https://doi.org/10.1016/S0377-0273(98)00101-2

Planet Team (2017). Planet application program interface: In space for life on Earth, *San Francisco, CA*, *2017*, 40.

Rolph, G., Stein, A., & Stunder, B. (2017). Real-time environmental applications and display system: READY. *Environmental Modelling & Software*, *95*, 210–228. https://doi.org/10.1016/j.envsoft.2017.06.025

Ryan, W. B., Carbotte, S. M., Coplan, J. O., O'Hara, S., Melkonian, A., Arko, R., et al. (2009). Global multi-resolution topography synthesis. *Geochemistry, Geophysics Geosystems*, *10*, Q03014. https://doi.org/10.1029/2008GC002332

Sato, H., Suzuki-Kamata, K., Sato, E., Sano, K., Wada, K., & Imura, R. (2013). Viscosity of andesitic lava and its implications for possible drain-back processes in the 2011 eruption of the Shinmoedake volcano. *Japan, Earth Planets and Space*, *65*, 13.